The Influence of Moment of Inertia-Based on Flight Nonlinear Simulation

Ali Mohamed Elmelhi
University of Tripoli
Electrical and Electronic Engineering Department
Faculty of Engineering
Po.Box. 13786
Tripoli, Libya
ali_elmulhi@yahoo.com

ABSTRACT: *The on line behavior of the flight vehicle can be described via nonlinear simulation of the equations of motions. Where, from the control point of view, this needed to test the trajectory performance before real flight. In this article, the simulation is carried out in order to design the suitable model for a desired nominal angle of attack trajectory, which satisfies some typical burnout parameters in active flight phase, and to test the robust performance of the longitudinal Autopilot when the moment of inertia dynamics are considered. Moreover, the nonlinearity due to saturation limits of actuator deflections is investigated. Simulation results are presented at the end of this paper, to show the effectiveness of nonlinear fuzzy Autopilot by comparing to the classical design approach, when the coupling uncertainty is considered.*

Keywords: Vehicle Dynamics, PID Controller, Fuzzy Controller, Missile Coupling, Moment of Inertia, Ballistic Trajectory Design

Received: 12 June 2012, Revised 28 July 2012, Accepted 4 August 2012

Nomenclature

m; Vehicle mass (kg) .

V; Vehicle relative velocity (m/sec).

T; Effective thrust (N).

α, β; Angle of attack and side slip angle(deg).

ρ; Air density ($kg - m^{-3}$).

S_a; Reference surface area (m^2).

C_x^α; Aerodynamic drag coefficient.

C_y^α; Aerodynamic left coefficient due to angle of attack.

g; Gravity acceleration (m/sec^2).

x_l, y_l;	Range and altitude in launch frame (m).
R;	Earth radius (6378140 m).
θ, ψ, and ϕ;	Euler angles [pitch, yaw and roll] (deg).
γ;	Flight path angle.
p, q and r;	Roll, pitch and yaw rates (deg/sec).
r_d;	Radius distance from earth center to the point considered in space (m) .
m_z^{α} and m_y^{β};	Moment coefficients due to angle of attack and side slip angles.
L_T;	Total vehicle length (m).
x_z;	The distance from theoretical tip of vehicle center of mass (m).
l_a;	Reference length (m).
m_z^q, m_z^r and m_y^p;	Moment coefficients due to pitch, yaw and roll rates.
z_r;	Distance between the longitudinal axis to the vibration pivot (m) .
δ_θ, δ_ϕ and δ_ψ;	Elevator, roll and yaw deflections (deg).
ω_x, w_y and w_z;	Angular velocities in roll, yaw and pitch channels (deg/sec^2).
μ_T;	Mass propellant flow rate (kg/sec)
$\boldsymbol{I_x}$;	Moment of Inertia in $\boldsymbol{x}$ axes ($\mathbf{m^2.sec}$).
$\boldsymbol{I_c}$;	Moment of inertia in $\boldsymbol{x, z}$ axes ($\mathbf{m^2.sec}$).

1. Introduction

The nonlinear rigid-body equations of motion were used to model the nonlinear flight dynamics in the form of translational and rotational motion [1, 2, 3, 4, 5]. These equations of motion are the basic concepts for presenting the mathematical model of the launch vehicle such as ballistic missile. The nonlinear simulation becoming a key stage in the analysis and design of control systems. In the field of flight control, the Autopilot design (simply being a control system used for flight control) is typically two stage process, with approximate linear analysis followed by an extensive set of nonlinear simulation to safely design of the Autopilot [6].

The nonlinear simulation is required her because the aerospace launch vehicles are highly nonlinear systems and their behaviors have to be tested before a real flight. The most significant phenomena of nonlinear behavior problem is due to actuator driving the control surfaces having deflections and rate of deflection limits. This discontinuous feature of the actuators often results in nonlinear Autopilots being designed so that the limits are never reached. Typically, for a missile Autopilot, the input is the demanded control surface deflection in three channels pitch, yaw and roll. The outputs are the achieved airframe angular accelerations and body angular rates measured about the body axes. Other output variables such as pitch, yaw, and roll angles can be derived from the longitudinal, lateral, roll accelerations and body rates. Actually, a high performance nonlinear Autopilot control designs based on fuzzy proportional controller [fuzzy PD] is considered here to achieve a high tracking performance [7 , 8, 9].

The first objective of this study is to build and simulate the nonlinear equation of motions for the considered launch vehicle, so that its behavior motion before hardware in loop simulation can be tested. This simulation is carried out with moment of inertia coupling dynamics are considered, which has been derived in [10]. Second is to design the desired nominal angle of attack model in order to satisfy some typical burnout parameters. Third, is to investigate the robustness of the fuzzy PD controller by comparing with classical PD, when the effect of moment of inertia coupling dynamics is considered. Finally, to avoid the nonlinear phenomena caused due to actuator deflection limits. This study can be accomplished according to the following sections: in section 2, the nonlinear model of the launch vehicle in three channels is described. In section 3, the mathematicalmodel for the angle of attack nominal trajectory is presented. In section 4, the Autopilot model using classical and fuzzy proportional controllers is included. In section 5, the computer simulation results are obtained. Finally the conclusion is written in section 6.

2. Nonlinear Model

In order to understand the physical motion of the space vehicle, the related conventions and notations of the body axes systems as well as the forces, moments and other quantities are shown in Figure 1.

In this study, suppose the system is a rigid body dynamics, and further suppose that the elasticity effects in the flexible body model are neglected. These assumptions are considered because the elastic high frequency bending modes are the limiting factor in obtaining a satisfactory stability margins in an Autopilot design [11]. Furthermore, the following simplifications are also considered:

- The earth is spherical and non-rotating.
- The launch vehicle is symmetrical so that only the force equations in longitudinal motion are considered.
- No effect of wind.

Accordingly, the following nonlinear equations of motions are obtained [12], [13] and [14]:

Force equation [axial force].

$$m\dot{V} = T\cos(\alpha) - 0.5\rho V^2 S_a C_x - mg\,((x_l/r_d)\cos(\gamma) + (((R + y_l)/r_d))\sin(\alpha)) \quad (1)$$

Normal force equation

$$mV\dot{\gamma} = T\sin(\alpha) - 0.5\rho V^2 S_a C_y^{\alpha}\alpha - mg\,((x_l/r_d)\sin(\gamma) + (((R + y_l)/r_d))\cos(\alpha)) \quad (2)$$

Angular acceleration equation in pitch plane

$$\dot{\omega}_z = 0.5\rho V^2 S_a l_a\, m_z^{\alpha}\alpha + (0.5\rho V^2 S_a l_a^2 / V) m_z^q q + (\mathrm{T}/\sqrt{2})\,(L_T - x_z)\,\delta_\theta)\,/\,I_c \quad (3)$$

Angular acceleration equation in yaw plane

$$\dot{\omega}_y = 0.5\rho V^2 S_a l_a m_z^{\beta}\beta + (0.5\rho V S_a l_a^2 / V) m_y^r r + (\mathrm{T}/\sqrt{2})\,(L_T - x_z)\,\delta_\psi)\,/\,I_c \quad (4)$$

Angular acceleration equation in roll plane

$$\dot{\omega}_x = 0.5\rho V S_a l_a^2\, m_x^p p + T z_r \delta_\phi)\,/I_x \quad (5)$$

Rate of change of pitch angle equation

$$\dot{\theta} = \omega_z \quad (6)$$

Rate of change of yaw angle equation

$$\dot{\psi} = \omega_y \quad (7)$$

Rate of change of roll angle equation

$$\dot{\phi} = \omega_x \quad (8)$$

Range equation

$$\dot{x}_l = V\cos(\gamma) \quad (9)$$

Altitude equation

$$\dot{y}_l = V\sin(\gamma) \quad (10)$$

Rate of change of propellant mass equation

$$\dot{m} = -\mu_T \quad (11)$$

Geometry relation equation

$$\alpha = \theta - \gamma \quad (12)$$

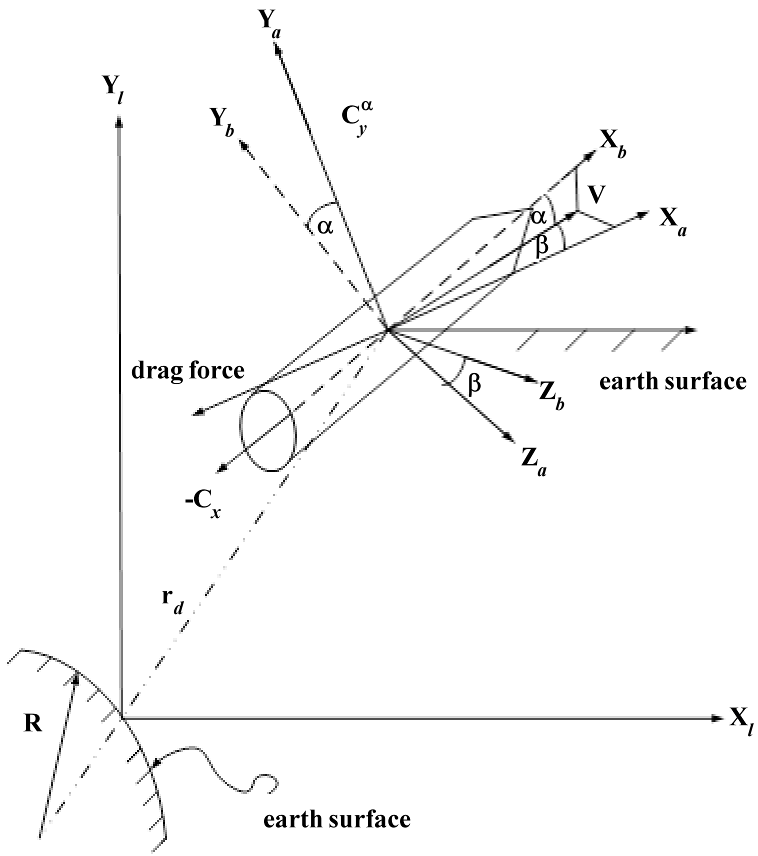

Figure 1. Vehicle geometry

In the above nonlinear equations of motion, the moment of inertia coupling dynamics are not included. These undesired dynamics are added separately via angular acceleration equations in pitch and yaw planes while have no effect on the roll motion.

Consequently, the (3) and (4) are modified as follows.

$$\dot{\omega}_z = 0.5\rho V^2 S_a l_a\ m_z^{\alpha}\alpha + (0.5\rho V^2\ S_a l_a^2 / V) m_z^q q + (\mathrm{T}/\sqrt{2})\,(L_T - x_z)\,\delta_\theta) - \mathbf{I_c} - \mathbf{I_x})\,\mathbf{W_x}\ \mathbf{W_y})/I_c \tag{13}$$

$$\dot{\omega}_y = 0.5\rho V^2 S_a l_a\ m_z^{\beta}\alpha + (0.5\rho V S_a l_a^2 / V) m_y^r r + (\mathrm{T}/\sqrt{2})\,(L_T - x_z)\,\delta_\psi) - \mathbf{I_c} - \mathbf{I_x})\,\mathbf{W_x}\ \mathbf{W_y})/I_c \tag{14}$$

For more details about the derivation of these coupling models, the reader refers to [10]. And it should be noted that, the moment of inertia in yaw and roll channels are identical ($I_y = I_z = I_c$) due to symmetrical configuration of the considered vehicle.

3. Desired Angle of Attack Model

The nominal desired angle of attack trajectory is applied here as a longitudinal tracking objective input. And the launch vehicles have to be stabilized around this trajectory until the burnout time [the time for the vehicle shutoff engine] is reached. The trajectory behavior of the angle of attack is selected in such way that the typical burnout parameters have to be achieved. Figure 2 shows an approximate sketch of the nominal trajectory of angle of attack at different phases. And the mathematical model in each phase can be designed as follows.

• **Vertical ascend phase [0 *to* t_1]**

$$\theta(t) = 90,\ \alpha_d(t) = 0,\ \dot{\gamma}(t) = 0,\ \gamma(t) = 90$$

• **Turning by air force and gravity phase [t_1 to t_2]**

$$(d\theta(t)/dt) < 0,\ \alpha_d(t) < 0,\ \dot{\gamma}(t) < 0$$

Where the variation of the angle of attack $\alpha_d(t)$ can be evaluated based on the following formula:

$$\alpha_d(t) = -a_{m1} sin^2 (f(t)) \tag{15}$$

And

$$f(t) = (\pi(t - t_1)) / (k(t_2 - t\ )) + (t - t_1)) \tag{16}$$

$$k = (t_{m1} - t_1 / t_2 - t_{m1}) \tag{17}$$

With t_m is the time corresponding to the Amplitude a_m

• **Turning by gravity phase [t_2 to t_3]**

$$(d\theta(t)/dt) < 0,\ \alpha_d(t) = 0,\ (d\gamma(t)/dt) < 0$$

• **Aiming phase [t_3 to t_4]**

$$\theta(t) = constsnt,\ \alpha_d(t) > 0,\ (d\gamma(t)/dt) < 0$$

And in this case, the variation of the angle of attack $\propto_d(t)$ is represented by

$$\propto_d(t) = a_{m2} sin^2 (f(t)) \tag{18}$$

And

$$f(t) = (\pi(t - t_3)) / (k(t_4 - t\ )) + (t - t_3)) \tag{19}$$

$$k = (t_{m2} - t_3) / (t_4 - t_{m2}) \tag{20}$$

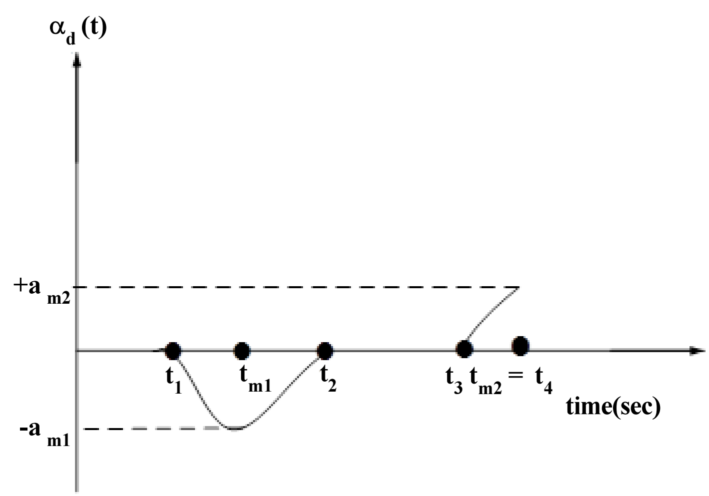

Figure 2. Approximate sketch of desired angle of attack trajectory $\alpha_d(t)$

In order to see the behavior of the longitudinal motion of a considered typical launch vehicle, the nonlinear equation of motions in the previous section, have to be simulated by adjusting the nominal command angle of attack according to the above four phases. It should be noted that, the main interesting direction of this work is to stabilize the system in longitudinal plane by pitching around this nominal trajectory as mentioned before.

4. Autopilot Model

4.1 Proportional Derivative Controller[PD]

One of the most widely used controllers in the design of continuous data control systems is the proportional integral derivative controller (PID) [15]. In this work for flight control stabilization, the part of this general controller called PD is selected due to interesting to keep a high tracking performance in the transient response specifications.

Figure 3 show the general block diagram of a continuous PD controller acting on an error signalh $e(t)$. The proportional controller multiplies $e(t)$ by a constant k_p and the derivative control generates a signal equal to k_d times the time derivative of $e(t)$. And the derivative controller provides an anticipatory action to reduce the overshoots and oscillations in the time response. This type of controller will be used to design three channels (pitch, yaw and roll) Autopilots. Where the generated PD control signal $u_{PD}(t)$ cause the flaps of the equivalent actuators such as elevators, rudders and ailerons to deflect, so that desired objective angles can be achieved. this signal can be expressed by the following differential equation:

$$u_{PD}(t) = k_p\, e(t) + k_d (de(t) / dt) \qquad (21)$$

In this appropriated linear classical design approach, the linearized vehicle model in three channels have to be derived and then the controller gains are designed at different operating points along the active or powered phases of flight trajectory. As a result, the gain scheduling for these gains in three channel Autopilots can be constructed. This procedure is required in order to apply this controller in nonlinear simulation. For robustness and to avoid the efforts for controller gains adjustment in each operating point on trajectory, an alternative nonlinear PD controller using fuzzy logic control [FLC] is considered here which will be briefly explained as in the following:

4.2 Fuzzy Controller

While conventional PD controller depends on the accuracy of the vehicle model and parameters in three channels, the FLC introduce different design approach. Where instead of using a system model, the operation of a FLC is based on heuristic knowledge and linguistic description to perform a task. In this design problem, the FLC is applied as PD controller to get a fuzzy controller called Fuzzy PD. The performance of this controller in each Autopilot channel is then improved by adjusting the rules and membership functions parameters. And the main useful based on this approach that, the controller parameters can by adjusted directly in online simulation of the given vehicle model, and without model linearization as in conventional PD controller design.

The procedures for fuzzy PD controller can be explained as follows.

• Defining inputs and universe of discourse

To apply heuristic knowledge in the FLC, inputs and universe of discourse are defined first. The inputs are the error $e(t)$ and change of error ($de(t)/dt$). And both of the input linguistic variables can be described on the universe of discourse by the following fuzzy set [NB, NM, NS, ZE, PS, PM, PB]. Where, NB denotes to Negative Big. NM; Negative Medium. NS; Negative Small. ZE; Zero. PS; Positive Small. PM; Positive Medium and PB represents a Positive Big.

• Defining the fuzzy membership functions

To perform fuzzy computation, the inputs are converted from the numerical or crisp value into linguistic forms. The term such as Small and Big are used to quantize the inputs values to linguistic values. Fuzzy membership functions are used as tools for fuzzification process. Fuzzy membership functions have contained several fuzzy sets depending on how many linguistic terms are used. Each fuzzy set represents one linguistic term. In this article, seven fuzzy sets are obtained by applying the seven linguistic terms as mentioned before. The number for indicating how much a crisp value can be a member in each fuzzy set is called a degree of membership. One crisp value can be converted to be partly in many fuzzy sets. But the membership function degree in each fuzzy set may be different.

The triangular membership functions are selected here to carrying out the fuzzification process due to their simplicity structure, symmetry and low computation time is required [16]. The model of these types of membership functions can be represented as inTable. 1 [17].

Left	$\mu^L(x) \begin{cases} 1 \\ max\left(0, 1 + \frac{c^L - x}{0.5w^L}\right) \end{cases}$	if $x \le c^L$ *otherwise*
Centers	$\mu^c(x) \begin{cases} max\left(0, 1 + \frac{x - c)}{0.5w}\right) \\ max\left(0, 1 + \frac{c - x)}{0.5w}\right) \end{cases}$	if $x \le c$ *otherwise*
Rights	$\mu^R(x) \begin{cases} max\left(0, 1 + \frac{x - c^R)}{0.5w^R}\right) \\ 1 \end{cases}$	if $x \le c^R$ *otherwise*

Table 1. Triangular membership model

Where c^L specifies the saturation point, W^L specifies the slope of the non-unity and nonzero part of μ^L. And similarly for μ^R. For μ^C. notice that c is the center of triangular and w is the base-width. The x variable here denoted to the inputs $e(t)$ or $(de(t)/dt)$.

• Rule base

For this vehicle control problem, with two inputs in each channel and seven linguistic values for every input, there are at most $7^2 = 49$ possible rules for only one channel. In general each rule can be represented by the following logic equation:

$$if\ \ e(t)\ is\ U_{e_j}\ \text{and}\ \dot{e}(t)\ U_{\dot{e}_j}\ \text{then}\ u_f(t)\ \text{is}\ u_{o_j} \tag{22}$$

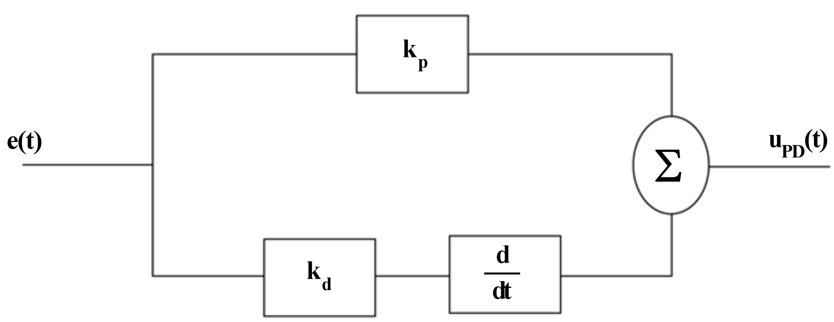

Figure 3. A continuous PD controller

Where $u_f(t)$ is the fuzzy (un-crisp) output signal, u_{o_j} represents the fuzzy output center rule. U_{e_j} and $U_{\dot{e}_j}$ represent respectively the certainty degree of the two input linguistic variables. In order to perform the inference mechanism, we must first quantify each of the rules with fuzzy logic as in the above equation. To do this, the meaning of premises of the rules ($e(t)$ is U_{e_j}) and ($\dot{e}(t)$ is $U_{\dot{e}_j}$).W which composed of several terms must be quantified [17]. And the quantification can be done via the triangular membership functions to combine the meaning of the two input linguistic variables. This can be yield by using of the minimum operation ($U_{e_j} \cdot U_{\dot{e}_j}$).W. Such type of process is called inference engine mechanism.

• Defuzzification process

This is the last stage in the fuzzy controller operation, in which the fuzzy signal is retransform again into crisp output signal. Similarly as mentioned before in conventional design, this reconstructed signal is applied to the vehicle actuators to get the desired deflections. In this study, the center of gravity method is chosen to carry out the defuzzification operation which can be represented by the following formula: [10], [7].

$$u^{crisp} = (\Sigma_i b_i \int \mu_{(i)}) / \Sigma_i \int \mu_{(i)} \tag{23}$$

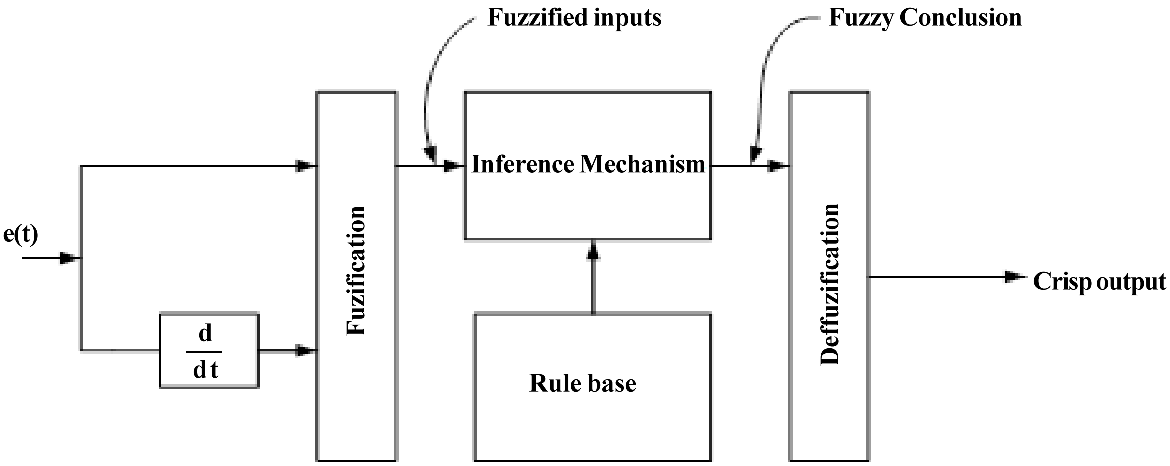

Figure 4. Fuzzy PD controller

Where, u^{crisp} denotes to the output crisp value, b_i is the fuzzy output rule centers and $\mu_{(i)}$ is the output of the minimum operation.

The general fuzzy PD controller system can be illustrated by the simplified general block diagram shown in Figure 4.

5. Simulation Results

Based on the propulsive, aerodynamic and geometry data for a typical launch vehicle [13] and [14], the computer simulation is carried out for the nonlinear equation of motion written in section 2.

The simulation results related to the longitudinal motion are considered here, and which related to the lateral and roll channel motions are ignored. This is because the stabilization of the vehicle in longitudinal motion is the main task of flight control engineer, and further to demonstrate the main objectives in this study.

5.1 Autopilot Design

The main objective of Autopilots in three channels [pitch, yaw and roll] is to control and stabilize of the vehicle body rates q, r and p, which have been designed by using of the classical and fuzzy PD controller. Consequently, the errors and change of errors in three channels are compensated to control the actuator deflections such as elevators, ailerons and rudders. However, due to actuators dynamics, the time delay in the compensated signals is caused and to overcome of this problem, their bandwidths should be large, so that their output responses can be enhanced. For this to be achieved, the whole actuator transfer functions are selected as a first order dynamics with a small time constant 0.01 *sec*. The block diagrams for three Autopilot loops in pitch, roll and yaw are shown in Figure 5. Where, the Autopilot block is simulated by two mentioned control design approaches.

• **Classical Autopilot design**

In order to verify and assess the performance of the fuzzy PD controller, the Autopilot design based on the classical PD controller is simulated for the aim of comparison. Where, the first issue for this objective is to linearize the nonlinear model includes the angular of moment equations written in (3), (4) and (5). And then by taking the Laplace transform operation, the following two transfer functions in s-domain are derived:

$$(\theta / \delta_\theta) = k_\theta / (s^2 + p_1 s + p_2) \tag{24}$$

$$(\phi / \delta_\phi) = k_\phi / (s - r_\phi) \tag{25}$$

Where, the yaw transfer function is ignored here due to a symmetrical configuration of pitch and yaw planes. And all the

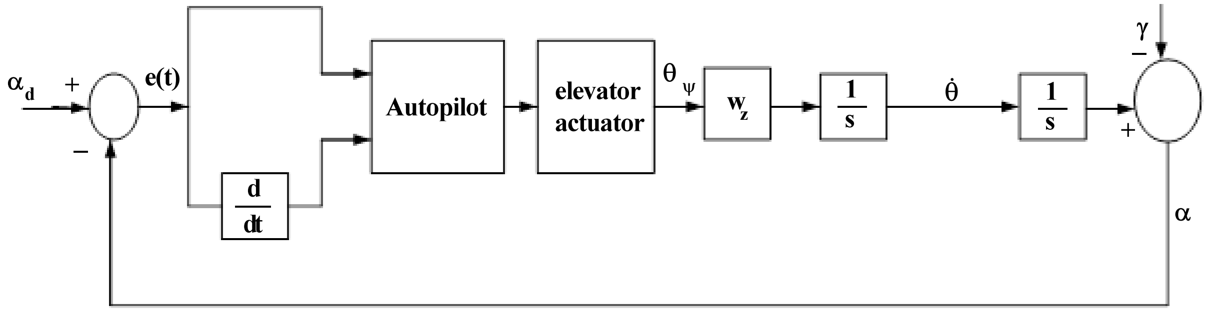

(a) Pitch Autopilot

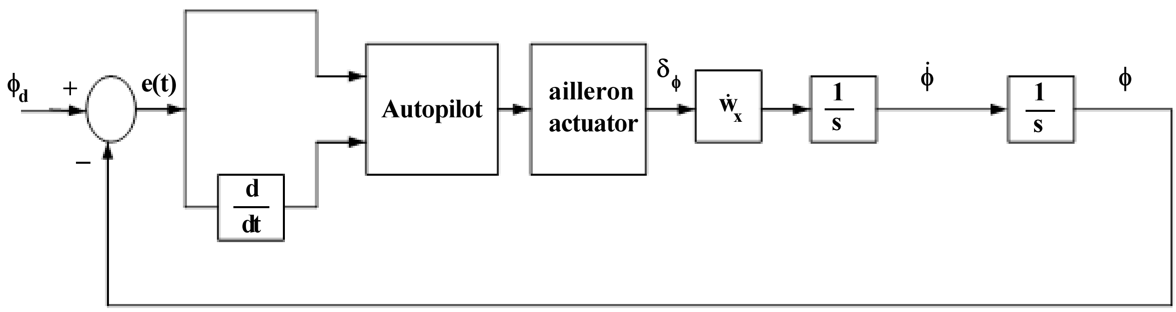

(b) Roll Autopilot

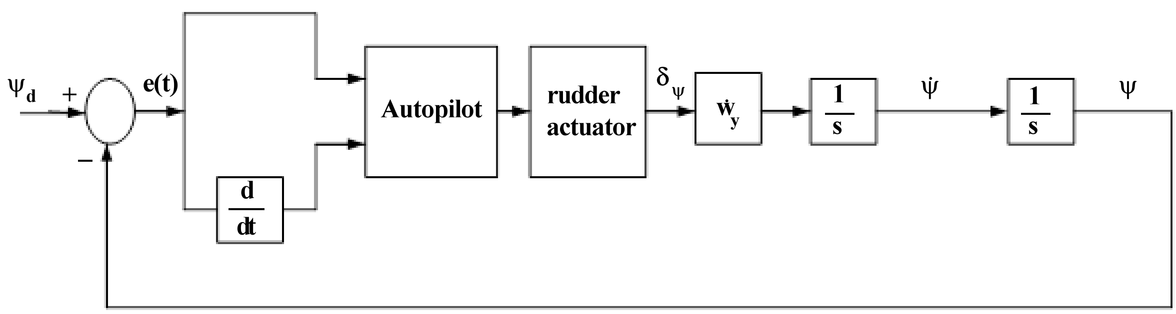

(c) Yaw Autopilot

Figure 5. Autopilot configurations in pitch, yaw and roll channels

unknown transfer functions parameters are rely on the aerodynamics and propulsive data which can be identified from the vehicle trajectory program at different instant of time [14] and [18]. These parameters can be expressed as

$$p_1 = (1/mV)\ \ Tcos(\alpha)\ +\ 0.5C_y^{\alpha}\rho V^2 S_a)\ \ -(0.5\ m_z^q \rho V S_a l_a^2\ / I_c) - (g / V)\, sin(\theta) \tag{26}$$

$$p_2 = (0.5\ m_z^q \rho V S_a l_a^2 / I_c)\,((g / V)\ \ sin(\theta)\ -\ (1/mV)\ =\ Tcos(\alpha)\ +\ C^{\alpha} q_d S_a)) - (0.5\ m_z^{\alpha} \rho V^2 S_m l_a\ ) / I_c \tag{27}$$

$$k_{\theta} = (0.5\ m_z^{\alpha} \rho V^2 S_m l_a) / I_c \tag{28}$$

$$r_{\phi} = (1 / I_x V)\,(0.5\ m_x^p \rho V^2 S_a l_a^2) \tag{29}$$

$$k_{\phi} = T z_r / I_x \tag{30}$$

Table 2 and Table 3 shows the controller gains for the conventional Autopilot PD controller in pitch and roll channels. Where, they have been designed at distinct operating points on the nominal flight trajectory. To obtain the compensated PD control

time	k_p	k_d
5 sec	18.49	4.584
10 sec	18.49	4.695
20 sec	18.649	4.646
30 sec	19.649	4.586
40 sec	20.0649	4.425

Table 2. Classical PD controller gains for pitch Autopilot

time	k_r	k_{dr}
5 sec	1.6431	0.244
10 sec	1.6431	0.2484
20 sec	1.6431	0.2514
30 sec	1.6431	0.2814
40 sec	1.411	0.3221

Table 3. Classical PD controller gains for roll Autopilot

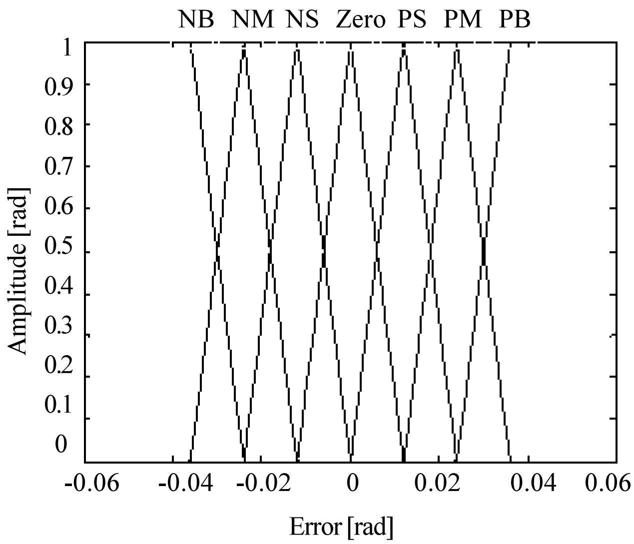

(a) Error membership functions

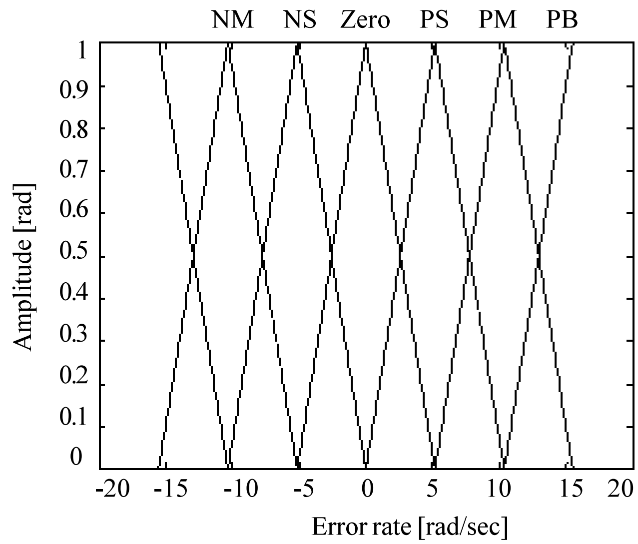

(b) Change of error membership functions

Figure 6. Triangular Membership Functions

$e(t)$ \ $de(t)/dt$	NB	NM	NS	ZERO	PS	PM	PB
NB	0.60	0.60	0.60	0.60	0.40	0.20	0
NM	0.60	0.60	0.60	0.40	0.20	0	-0.20
NS	0.60	0.60	0.40	0.20	0	-0.20	-0.40
ZERO	0.60	0.40	0.20	0	-0.20	-0.40	-0.60
PS	0.40	0.20	0	-0.20	-0.40	-0.60	-0.60
PM	0.20	0	-0.20	-0.40	-0.60	-0.60	-0.60
PB	0	-0.20	-0.40	-0.60	-0.60	-0.60	-0.60

Table 4. Fuzzy rule base centers for pitch Autopilot

error signal, the adjusted gains are interpolated over whole flight time until the burnout.

• Fuzzy Autopilot design

This designed is accomplished by constructing the symmetrical membership functions for the error and change of error, in addition to the rule base centers. The triangular membership functions based on the model written in Table 1 have been built by

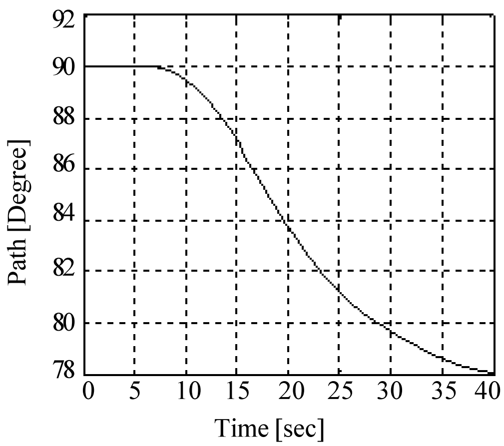

(a) Path angle

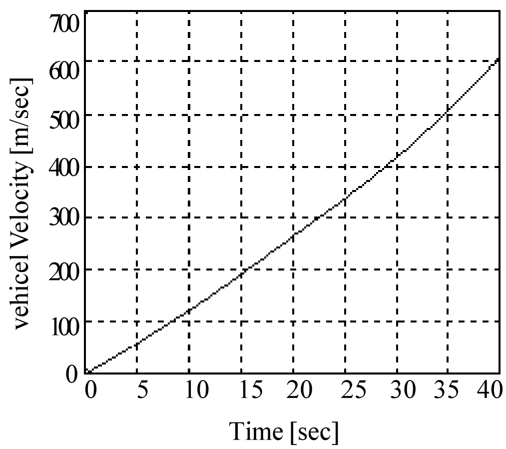

(b) Vehicle velocity

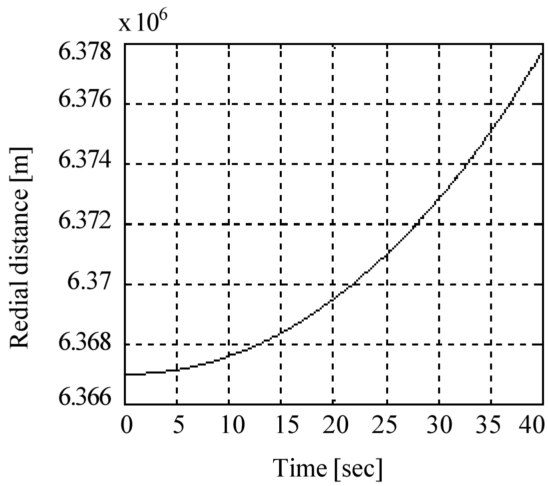

(c) Radial distance

Figure 7. Burnout parameters using classical PD Autopilot

adjusting their widths and centers until the required tracking performance for the desired angle of attack is achieved. Moreover, the centers of the rule base table have to be adjusted so that the tracking performance is improved.

Table 4 shows the two dimensional rule base for the longitudinal control motion. The central portion of the rule base makes use of the entire output of the universe of discourse. This is the position where the outputs from the error [difference between input desired angle of attack and actual angle of attack] and its derivative are substituted by the equivalent linguistic variable within the designed universe of discourse. After adjusting the fuzzy PD controller, the final membership functions and rules are obtained respectively as shown in Figure 6 and Table 4. It is seen that, the designed range of the universe of discourse for the position error and change of error are respectively given by [-0.36,0.36] and [-15.01, 15.01].

5.2 Nonlinear Simulation Results

As mentioned before, the longitudinal Autopilot forces the vehicle in the direction of the given nominal angle of attack trajectory. This trajectory has been obtained by simulating the distinct turning model phases in section 3. Where the related parameters are adjusted until the burnout parameters such as vehicle speed, radial distance and flight path angle are demonstrated. The designed parameters for the angle of attack trajectory are given as follow.

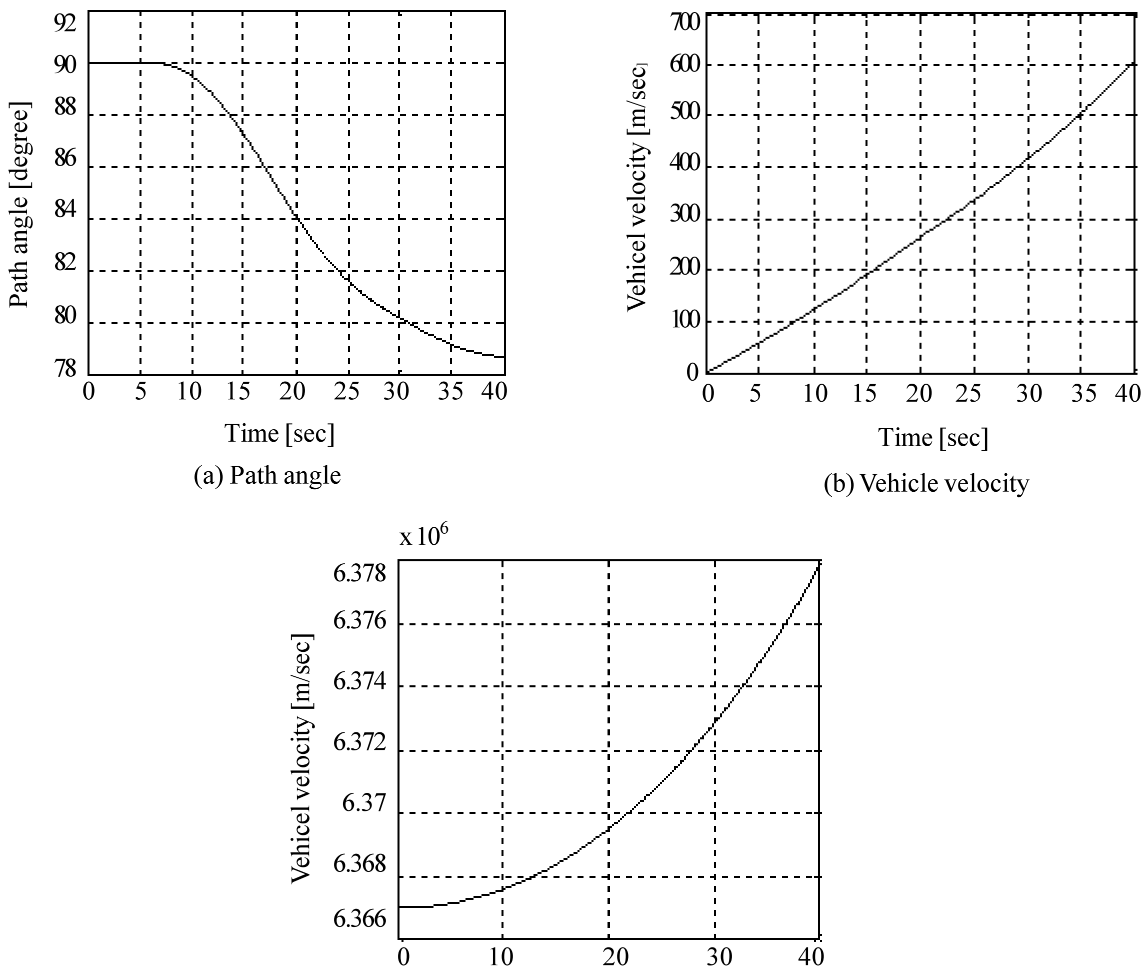

(a) Path angle

(b) Vehicle velocity

(c) Radial distance

Figure 8. Burnout parameters using Fuzzy PD Autopilot

Design method	Pitch rate[deg/sec]	Deflection [deg]
Classical PD	Maximum: -12.63 Minimum: -22.7	Maximum: 89.03 Minimum: 5.804
Fuzzy PD	Maximum: -0.95 Minimum: 0.224	Maximum: -1.844 Minimum: 0.834

Table 5. Numerical results

$t_1 = 5\ sec, t_2 = 30\ sec, t_3 > 30\ sec, t_4 < 45\ sec, t_{m1} = 18\ sec, a_{m1} = 0.0698, k = 1.0833, a_{m2} = 0.035, t_{m2} = 40\ sec$

• **Burnout simulation results**

The trajectories behavior of these burnout parameters based on classical and fuzzy PD Autopilots are shown respectively by Figure 7 and Figure 8. Where the radial distance is evaluated by the following mathematical equation:

$$r_d^2 = x_l^2 + (R + y_l)^2 \tag{31}$$

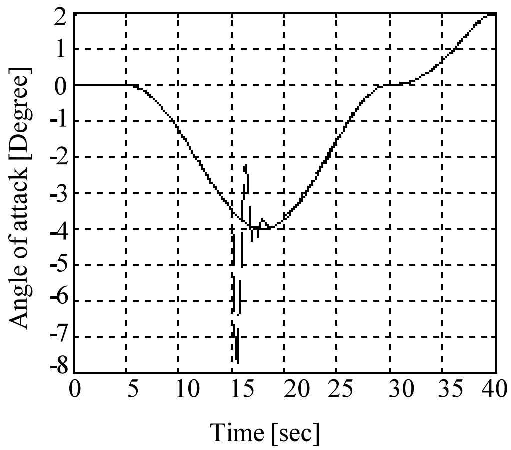

(a) Angle of attack trajectory

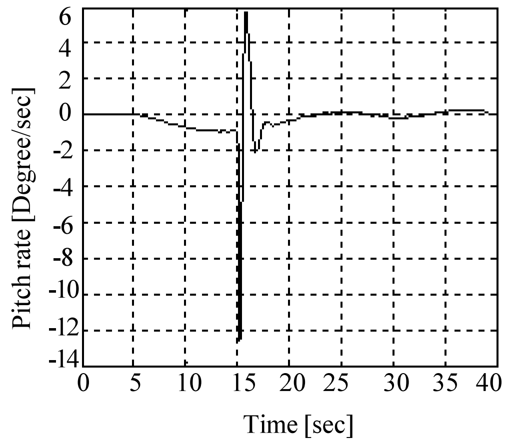

(b) Pitch rate

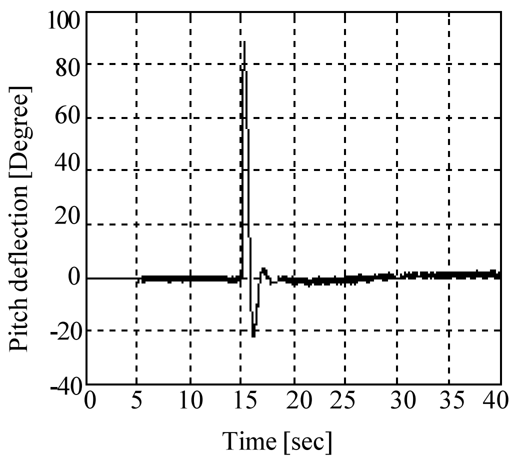

(c) Pitch elevator deflection

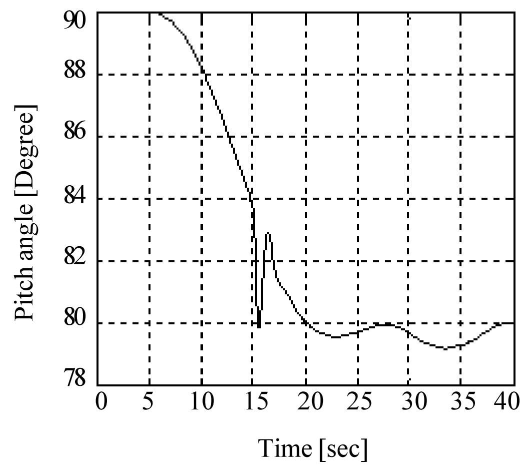

(d) Pitch angle trajectory

Figure 9. Effect of moment of inertia using classical PD Autopilot

From these results, the values of the burnout parameters are approximately equal in both design techniques, and a little difference is observed in case of flight path angle due to exist of the inertia coupling.

• Influence of moment of inertia coupling

It is known that, the fuzzy logic controllers have succeeded in many control problems that conventional control theories have difficulties to deal with. This can be demonstrated from the trajectory simulation of the nominal and actual angle of attack, when the influence of moment of inertia is considered. In this simulation, both the classical and fuzzy PD Autopilots are applied here in order to sta*b*ilize *the* considered vehicle, and to test the robust performance of each design approach. The simulation results are shown in Figure 9 and Figure 10 in which the solid lines for angle of attack trajectory denote to the desired nominal angle, and dashed lines are related to the actual output angle.

It is clear that, both design methods are successful for tracking of a desired command angle of attack until the burnout time (t = 40 *sec*) is reached. However, when the moment of inertial coupling is applied at time (t = 15 *sec*), the fuzzy controller can keep a better tracking at this moment of time, where a significant overshoot is observed in case of conventional design approach as shown respectively in Figure 10-a and Figure 9-a. At the same instant of time, and in contrast to conventional design technique, the distortion of the pitch angle due to such type of coupling can be avoided in case of fuzzy PD Autopilot as shown respectively in Figure 9-d and Figure 10-d. And by using Autopilot fuzzy design technique, a minimum pitch rate is observed as shown in Figure10-b in comparing to classical design shown in Figure. 9-b. Furthermore, in comparing to classical Autopilot, a

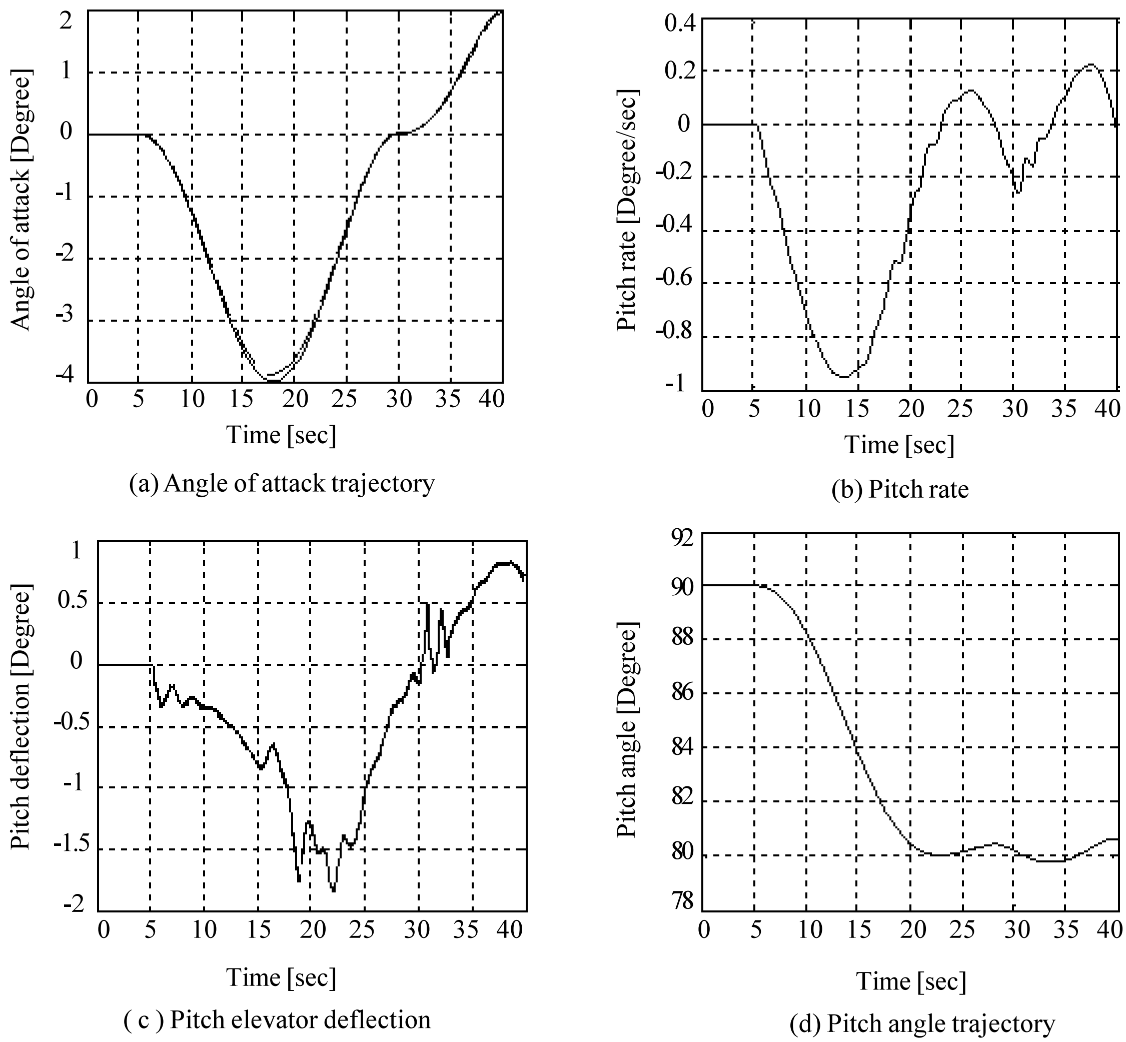

Figure 10. Effect of moment of inertia using fuzzy PD Autopilot

fewer amount of elevator deflection can be achieved as shown respectively in Figure. 9-c and Figure.10-c. As a result, the saturation nonlinearity due to actuator deflection limits can be overcome in case of fuzzy Autopilot. The range of pitch rate and elevator deflections for both design approaches is shown in Table. 5.

6. Conclusion

The nonlinear equations of motions for a typical launch vehicle model have been considered. And this nonlinear model is simulated with the influence of moment of inertia coupling. The angle of attack nominal trajectory model is presented and the burnout parameters have been obtained. In this study, the Autopilot is designed based on classical and fuzzy proportional derivative controllers, where their effectiveness in nonlinear simulation is investigated. Based on this study, it is concluded that, the Autopilot via fuzzy controller can achieve a better tracking performance without significant overshoot is observed, and minimum pitch rate can be achieved. Furthermore, the limiting factor due to saturation nonlinearity of an elevator deflection can be overcome.

References

[1] Stevens, B. L., Lewis, F. L. (1992). *Aircraft Control and Simulation.* John Wiley & Sons,Inc., New York, NY.

[2] Morelli, E. A. (2000). Airplane Flight Mechanics - Stability and Control. Class Notes.

[3] Schmidt, L.V. (1998). Introduction to Aircraft Flight Dynamic*s*. American Institute of Aeronautics and Astronautics, Inc., Reston, VA.

[4] Cook, M. V. (1997). Flight Dynamics Principles*.* John Wiley & Sons Inc., New York, NY.

[5] Etkin, B., Reid, L. D. (1996). Dynamics of Flight, Stability and Control*.* 3rd Ed., John Wiley & Sons, Inc., New York, NY.

[6] Fielding.c., Varaga. A., Bennani. S., Selier. M. (2002). Advanced techniques for clearance of flight control laws. Springer. Verlage, New York.

[7] Zadeh. L. A. (1965). Fuzzy Sets. *Information and Control*. 8, 338-353.

[8] Lee, C. C. (1990). Fuzzy Logic in Control Systems: Fuzzy Logic Controller Part I. *IEEE Trans. Syst.Man.Cyb*, 20, 404-418.

[9] Lee C. C. (1990). Fuzzy Logic in Control Systems: Fuzzy Logic Controller Part II. *IEEE Trans. Syst.Man.Cyb*, 20, 419-435.

[10] Ali ELMELHI. (2012). Flight Coupling Model Effect Based Fuzzy Control Logic. INTECH 2012, Morocco, 426-432.

[11] DITEm, W. A., Freed, L.E., Lanzer, L. F. (1958). Stage I Autopilot Design Study. WS107A-2, Series I, Lot B, Space Techn. Lab. Rep. GM-TN-0165-00139.

[12] Arthur, L., Greensite. (1970). Analysis and Design of Space Vehicle Flight Control System. copyright by Spartan books, printed in USA.

[13] Xiao. Ye. Lun. (2002). Rocket Ballistics and Dynamics. Class Lecture Notes, Beijing University of Aeronautics and Astronautics, Beijing.

[14] Tahir. Mustafa. (2003). Flight Program Design and Trajectory Optimization of a Ballistic Missile. Master thesis, Biejing University of Aeronautics and Astronautics.

[15] Kuo. B. C. (1991). Automatic Control Systems. 6th ed., Prentice – Hall, Englewood cliffs, N.J.

[16] Yodyium Tipsuwan., Mo-Yuen Chow. (1999). Fuzzy Logic Microcontroller Immplementation for DC Motor Speed Control. *In*: IEEE, *p*.1271-1276.

[17] Kevin M. Passino., Stephen Yurkovich. (1998). Fuzzy Control. Addison Wesley Longman. Inc, Copyright c.

[18] Ali. Mohamed. Elmelhi. (2005). Flight Vehicle's Stabilization Based Fuzzy Logic Control Design and Optimization. ph. d thesis, Biejing University of Aeronautics and Astronautics, Biejing, china.